Cross-talk of insulin-like peptides, juvenile hormone, and 20-hydroxyecdysone in regulation of metabolism in the mosquito *Aedes aegypti*

Lin Ling[a,b] and Alexander S. Raikhel[a,b,1]

[a]Department of Entomology, University of California, Riverside, CA 92521; and [b]Institute of Integrative Genome Biology, University of California, Riverside, CA 92521

Contributed by Alexander S. Raikhel, December 30, 2020 (sent for review November 11, 2020; reviewed by Naoki Okamoto, Subba Reddy Palli, and Kim Rewitz)

Female mosquitoes feed sequentially on carbohydrates (nectar) and proteins (blood) during each gonadotrophic cycle to become reproductively competent and effective disease vectors. Accordingly, metabolism is synchronized to support this reproductive cyclicity. However, regulatory pathways linking metabolism to reproductive cycles are not fully understood. Two key hormones, juvenile hormone (JH) and ecdysteroids (20-hydroxyecdysone, 20E, is the most active form) govern female mosquito reproduction. *Aedes aegypti* genome codes for eight insulin-like peptides (ILPs) that are critical for controlling metabolism. We examined the effects of the JH and 20E pathways on mosquito ILP expression to decipher regulation of metabolism in a reproducing female mosquito. Chromatin immunoprecipitation assays showed genomic interactions between *ilp* genes and the JH receptor, methoprene-tolerant, a transcription factor, Krüppel homolog 1 (Kr-h1), and two isoforms of the ecdysone response early gene, E74. The luciferase reporter assays showed that Kr-h1 activates *ilps 2*, *6*, and *7*, but represses *ilps 4* and *5*. The 20E pathway displayed the opposite effect in the regulation of *ilps*. E74B repressed *ilps 2* and *6*, while E74A activated *ilps 4* and *5*. Combining RNA interference, CRISPR gene tagging and enzyme-linked immunosorbent assay, we have shown that the JH and 20E regulate protein levels of all eight *Ae. aegypti* ILPs. Thus, we have established a regulatory axis between ILPs, JH, and 20E in coordination of metabolism during gonadotrophic cycles of *Ae. aegypti*.

insulin | hormone | insect | metabolism | CRISPR-Cas9

Mosquito-borne diseases continue to emerge and reemerge globally (1). For some viral pathogens, the lack of vaccines places a greater emphasis on disease prevention through effective mosquito management and control (1, 2). The *Aedes aegypti* mosquito is the major vector involved in transmission of human arboviral diseases such as dengue, chikungunya, yellow fever, Zika virus, and others (3–6). The World Health Organization (WHO) and Centers for Disease Control and Prevention (CDC) state that mosquitoes, particularly those from the genera *Aedes*, *Culex*, and *Anopheles*, continue to be organisms of utmost concern in global public health.

Disease-vector female mosquitoes undergo a biphasic feeding pattern, shifting from carbohydrates (nectar) to proteins (vertebrate blood) for survivorship, reproduction, and pathogen transmission (7, 8). Interchanging titers of juvenile hormone (JH) and 20-hydroxyecdysone (20E) shape the mosquito reproductive cycle (8, 9). JH-III (JH) controls the posteclosion (PE) phase, during which a female mosquito undergoes preparatory development for subsequent blood feeding and egg maturation. 20E controls the postblood-meal (PBM) phase from blood feeding to oviposition. These two phases form the gonadotrophic cycle in anautogenous mosquitoes. Methoprene-tolerant (Met), a basic helix–loop–helix (bHLH)-Per-Arnt-Sim (PAS) transcription factor, has been identified as the JH receptor (10–12). Additionally, a steroid receptor coactivator (Taiman) forms a heterodimer with Met to transduce the JH signal (13, 14). In the nucleus, the JH receptor complex activates target genes directly by binding a 9-mer Met-motif ($CACG^{C}/_{T}G^{A}/_{G}{}^{T}/_{A}G$); it also represses target genes indirectly, which requires other downstream factors (15, 16). Krüppel-homolog 1 (Kr-h1) is a C2H2 zinc-finger transcription factor that mediates Met action, either activating or repressing JH target genes by direct interaction with their Kr-h1-binding motifs (17, 18). The 9-mer sequence variations have been identified in *Ae. aegypti* as the Kr-h1-binding motif, which are similar to those first reported in *Bombyx mori* (16, 19).

A heterodimer of the ecdysone receptor (EcR) and ultraspiracle (USP) mediates 20E signaling to trigger a vast transcriptional program (20). The 20E receptor complex regulates target genes by means of either pseudopalindromic response elements resembling inverted repeats of AGGTCA separated by a single nucleotide spacer or downstream responsive genes (21). The ecdysone-inducible early gene E74 (*Eip74EF*) encodes an ETS (erythroblast transformation specific) transcription factor that mediates the 20E response in gene regulation. In mosquitoes, there are two isoforms, E74A and E74B, that act by differentially activating or repressing 20E-responsive genes (22, 23). They share a common C-terminal ETS DNA-binding domain and bind to a consensus core motif $^{C}/_{A}$GGAA, but have unique

Significance

In hematophagous female mosquitoes, each reproductive cycle is linked to a separate blood intake, serving as a foundation for the transmission of dangerous human diseases. During each reproductive cycle, female mosquitoes sequentially feed on carbohydrates and protein (blood). Metabolic flux is alternated to support the reproductive cyclicity. We have established that insulin-like peptides (ILPs), critical for regulating metabolism, are genetically controlled by juvenile hormone (JH) and 20-hydroxyecdysone (20E), the key hormones governing the reproduction of female mosquitoes. CRISPR gene-tagging experiments revealed that the JH and 20E pathways coordinate the production of ILPs. This study has uncovered the link between ILPs and JH and 20E pathways in controlling mosquito metabolism during reproduction of the *Aedes aegypti* mosquito.

Author contributions: L.L. and A.S.R. designed research; L.L. performed research; L.L. contributed new reagents/analytic tools; L.L. and A.S.R. analyzed data; and L.L. and A.S.R. wrote the paper.

Reviewers: N.O., University of Tsukuba; S.R.P., University of Kentucky; and K.R., University of Copenhagen.

The authors declare no competing interest.

[1]To whom correspondence may be addressed. Email: alexander.raikhel@ucr.edu.

This article contains supporting information online at https://www.pnas.org/lookup/suppl/doi:10.1073/pnas.2023470118/-/DCSupplemental.

Published February 1, 2021.

N-terminal sequences (23, 24). Moreover, E74 isoforms are differentially expressed in the *Ae. aegypti* mosquito (23).

Insulin-like peptides (ILPs) are pleiotropic peptide hormones encoded by multigene families that regulate metabolism, growth, reproduction, and longevity (25). The insulin signaling pathway is evolutionarily conserved (26). As many as 1 to 38 ILPs have been identified in insects (26). Even different mosquito species have varying numbers of ILPs (25). The model insect *Drosophila melanogaster* has eight ILPs (DILPs) (26). The production and release of DILPs are controlled by several different mechanisms, including nutrient sensing, neuropeptides, neurotransmitters or factors originating from the intestine, and adipocytes (26). After release, the action of DILPs can be modulated by hemolymph proteins that act either as protective carriers or competitive inhibitors (26). However, a species-specific and stage-dependent outcome with the control of the whole set of ILPs remains to be investigated.

Like *D. melanogaster*, the *Ae. aegypti* genome carries eight *ilps* that are expressed in the brain and other tissues (27). CRISPR-Cas9 analyses have shown that ILPs in this mosquito play different roles in body size determination and lipid metabolism (28, 29). Previous studies have revealed the involvement of JH and 20E pathways in the coordination of lipid and carbohydrate metabolism during the mosquito gonadotrophic cycle (30, 31). Here, we identified the functional link of JH and 20E pathways with eight ILPs in the control of mosquito metabolism.

Results

Tissue Distribution and Expression Patterns of ILPs in the Female *Ae. aegypti* Mosquito. We first determined the tissue localization of all eight *Aedes ILP* transcripts by means of quantitative real-time PCR (qPCR) analysis. This revealed differential distribution of *ILP* transcripts in female mosquito tissues. *ILPs 1*, *3*, *4*, *7*, and *8* were found to be brain specific. However, three other *ILPs* showed distribution in other tissues: *ILP2* transcripts were enriched in the ovary, *ILP5* in the carcass void of the fat body, and *ILP6* in the isolated fat body (Fig. 1). Next, we collected female mosquito tissues at five time points during the gonadotrophic cycle: 12 h and 48 h PE and at 12 h, 24 h, and 48 h PBM. Transcript levels of *ILPs 4* and *7* were high at 12 h PE and lower thereafter; the *ILP6* transcript had its peak at 48 h PE. Transcript levels of five other *ILPs* were higher during the PBM phase (*SI Appendix*, Fig. S1). The *ILP2* transcript exhibited a peak at 12 h PBM, and *ILPs 1*, *3*, *5*, and *8* at 24 h PBM (*SI Appendix*, Fig. S1). These expression patterns of the *ilp* genes suggest a possible link to the hormonal regulatory axis governed by JH and 20E.

JH and 20E Pathways Are Involved in the Regulation of *ilp* Gene Expression. Lipids and glycogen are the major energy reserves stored in the mosquito fat body, an insect analog of the vertebrate liver and adipose tissue (32, 33). JH and 20E have been implicated in the expression control of expression of genes coding for carbohydrate and lipid metabolic enzymes in the female *Ae. aegypti* (30, 31). To investigate the possibility of a direct effect of JH and 20E on the expression of metabolic enzyme genes, we conducted chromatin immunoprecipitation (ChIP) analysis. This revealed no genomic interaction between the JH (Met and Kr-h1) or the 20E (EcR and E74) pathway and selected metabolic genes (*SI Appendix*, Figs. S2–S4). Therefore, we hypothesized that JH and 20E might be involved in the cross-talk with other regulators of metabolism.

The role of insulin and ILPs in regulating metabolism is well established (25, 26). To determine a possible interaction of ILPs with the JH pathway in female mosquitoes, we first performed topical JH treatment. JH III (a 0.3-μL aliquot of 1 μg/mL) or acetone (control) was applied onto the abdomens of female mosquitoes at 6 h PE, when the level of this hormone is very low, and then the transcript levels of each of the eight *ILPs* was measured using RT-qPCR at 24 h post-JH application. The transcripts for *ILP2*, *ILP6*, and *ILP7* were significantly higher, while those for *ILP1*, *ILP3*, *ILP4*, *ILP5*, and *ILP8* were lower in JH III-treated mosquitoes than in controls (*SI Appendix*, Fig. S5*A*). The effect of *Met* RNAi was opposite: transcripts of *ILP2*, *ILP6*, and *ILP7* were down-regulated and those of *ILP1*, *ILP3*, *ILP4*, *ILP5*, and *ILP8* were up-regulated (Fig. 2*A*). Studies have shown that Kr-h1 is the key factor that mediates Met action in both activation and repression of JH-regulated genes (16, 18). After *Kr-h1* RNAi, transcripts of *ILP2*, *ILP6*, and *ILP7* were down-regulated, while *ILP1*, *ILP3*, *ILP4*, *ILP5*, and *ILP8* were up-regulated in a manner similar to that of *Met* RNAi (Fig. 2*A*).

To investigate whether *ilps* were transcriptionally responsive to the 20E pathway, we performed RNAi of *EcR* and *E74* and measured *ILP* transcript levels using RT-qPCR. Levels of *ILP2* and *ILP6* transcripts increased while those of *ILP4* and *ILP5* reduced in response to the *EcR* knockdown (Fig. 2*B*). Similar results were observed for RNAi of *E74*, demonstrating the

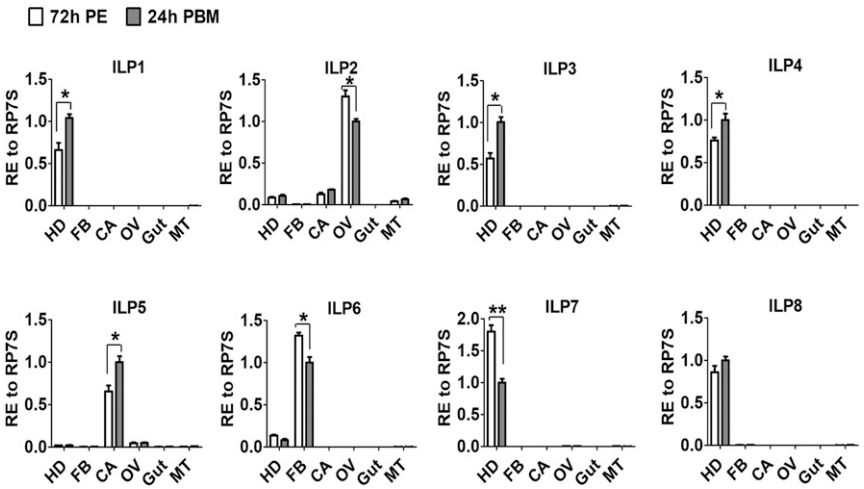

Fig. 1. Tissue distribution of *ILP* transcription in female *Ae. aegypti* mosquitoes. Relative expression levels of *ilp* genes in the head (HD), isolated fat body (FB), carcass (CA, abdominal wall without the fat body), ovary (OV), gut, and Malpighian tube (MT) at 72 h PE and 24 h PBM. Relative expression levels in abundant group at 24 h PBM are represented as 1, with corresponding adjustments in other values. Data represent three biological replicates with 30 individuals in each and are shown as mean ± SEM $*P < 0.05$, $**P < 0.01$.

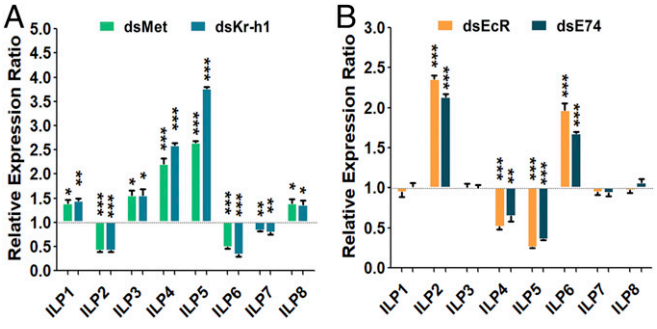

Fig. 2. Comparative analysis of *ILP* transcript abundance in *dsMet*, *dsKr-h1*, *dsEcR*, and *dsE74* RNAi female mosquitoes. (*A*) RNAi knockdowns of *Met* and *Kr-h1* repressed *ILP 2*, *6*, and *7* transcripts but activated the other five *ILPs*. (*B*) Knockdowns of *EcR* and *E74* elevated *ILP 2* and *6* transcripts, down-regulated *ILP 4* and *5*, while displaying no significant effect on the other *ILPs*. *dsLuc* (RNAi-*luciferase*) was used as control. Data represent three biological replicates with 30 individuals in each and are shown as mean ± SEM $*P < 0.05$, $**P < 0.01$, $***P < 0.001$.

indispensable role of E74 in conveying the 20E-EcR/USP signaling in regulating the *ilp* genes (Fig. 2*B*). However, except for *ILP4*, the brain-specific *ILPs 1*, *3*, *7*, and *8* were unaffected, suggesting that 20E signaling modulates mainly those expressed in peripheral tissue *ILPs* (Fig. 2*B*). It is also possible that the brain-specific *ILPs* lack responsiveness due to a poor penetrance of dsRNAs into the mosquito brain.

Injection of 20E (0.3-μL aliquot of 500 ng/mL) induced a decline of the *ILP2* transcript levels and an elevation of transcripts of *ILP4* and *ILP5* (*SI Appendix*, Fig. S5*B*). No response to 20E was detected for transcripts of *ILPs 1*, *3*, *7*, and *8*. The effect of exogenous 20E on *ILP6* expression was not as clear cut as that elicited by *EcR* or *E74* knockdown (*SI Appendix*, Fig. S5*B*). Notably, the other factors of the insulin pathway displayed no changes in transcription after either of the above-mentioned RNAi treatments (*SI Appendix*, Fig. S6). Taken together, these data suggest that the JH and 20E influence *ilp* gene expression in the reproducing female mosquitoes.

Regulatory Interactions of *ilp* Gene Promoters with Met and Kr-h1. A single Met binding site was found only in the *ilp6* gene promoter (*SI Appendix*, Fig. S7). However, Kr-h1 binding motifs were identified in the 5′ upstream regulatory regions of all eight *ilp* genes (*SI Appendix*, Fig. S7). To determine whether Met and/or Kr-h1 confer their binding on *ilps*, we performed ChIP analysis followed by qPCR to specifically amplify Met- and Kr-h1-bound regions. The Met binding was detected only at the *ilp6* gene promoter, and *Met* RNAi depletion diminished this binding enrichment, confirming the authenticity of the Met binding (*SI Appendix*, Fig. S8). Kr-h1 binding was enriched not only at JH-activated genes—*ilps 2*, *6*, and *7*—but also at JH-inhibited genes—*ilps 4*, *5*, and *ilp8-ilp1-ilp3*. *Kr-h1* RNAi abolished these binding enrichments (*SI Appendix*, Fig. S9). To gain further confirmation of Met and Kr-h1 interaction with *ilp* genes, the dual-luciferase assay was performed in *D. melanogaster* S2 cells. The 1-kb 5′ upstream regulatory regions of the *ilp* genes harboring the Met and/or Kr-h1 binding motif sites were subcloned into the firefly luciferase reporter vector pGL3basic (*ilp-Fluc*). When the *ilp6-Fluc* plasmid was cotransfected with the *pAc-Met-Myc* and *pAc-Taiman-Flag* expression plasmids into S2 cells, the luciferase activity in the presence of JH III was more than 4.5-fold higher than in the control group transfected with only *ilp6-Fluc* (Fig. 3*A*). Next, we cotransfected reporter plasmids for each of eight *ilps* together with the *pAc-Kr-h1-Myc* expression vector. An elevation of luciferase activity was observed after cotransfection of *ilp2-Fluc*, *ilp6-Fluc*, and *ilp7-Fluc* with the *pAc-Kr-h1-Myc* expression vector; in contrast, there was a reduction after cotransfection of *ilp4-Fluc*, *ilp5-Fluc*, or *ilp8-1-3-Fluc* with *pAc-Kr-h1-Myc* (Fig. 3 *B* and *C* and *SI Appendix*, Fig. S10*A*). These responses are consistent with results from the JH treatment assay (*SI Appendix*, Fig. S5*A*). Furthermore, these changes in the luciferase activity were abolished after mutation of their binding motifs in *ilp* promoters (Fig. 3 *A*–*C* and *SI Appendix*, Fig. S10*A*).

The Regulatory Relationships of the *ilps* Genes with EcR and E74 Transcription Factors. The ChIP assays were conducted to elucidate whether there is any interaction of EcR with *ilp* gene promoters. This yielded no binding reaction between EcR and any

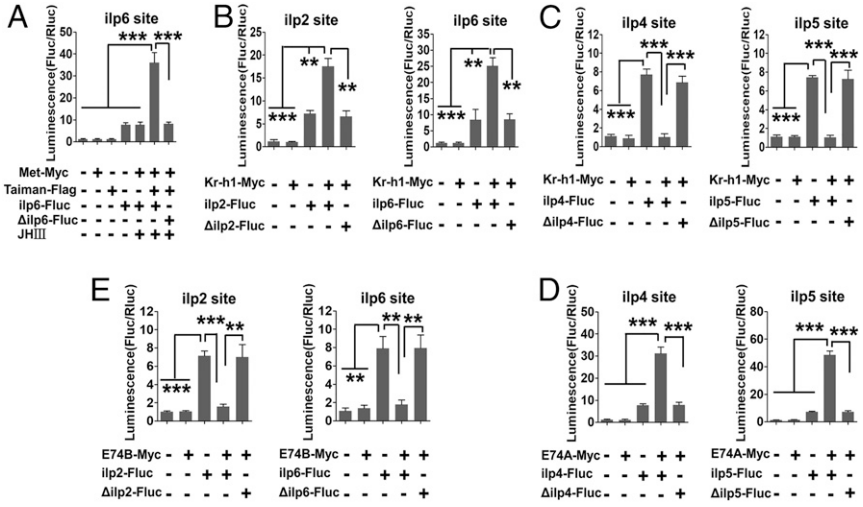

Fig. 3. Met, Kr-h1, E74A, and E74B regulate the transcription of *ilp* genes. (*A*) Luciferase reporter assay after cotransfection of expression vectors *pAc-Met-Myc* and *pAc-Taiman-Flag*, along with the reporter construct and JH III, indicates that Met is an activator of *ilp6* gene transcription. (*B*) Luciferase reporter assay after cotransfection of the expression vector *pAc-Kr-h1-Myc* and reporter constructs points out the activation role of Kr-h1 in the transcription of *ilps 2* and *6*. (*C*) Luciferase reporter assay shows that Kr-h1 is a repressor of the transcription of *ilps 4* and *5*. (*D*) Luciferase reporter assay after cotransfection of expression vectors *pAc-E74A-Myc* and reporter constructs indicates that E74A is a transcription activator of *ilp4* and *ilp5* genes. (*E*) Luciferase reporter assay after cotransfection of expression vectors *pAc-E74B-Myc* and reporter constructs indicates E74B as a repressor of *ilps 2* and *6* transcription. Treatments with the empty expression vector and no input DNA and motif mutation served as controls. Data represent six replicates and are shown as mean ± SEM $**P < 0.01$, $***P < 0.001$.

ilp gene throughout 3 kb of their 5′ upstream regulatory regions, indicating that the regulation of all eight *ilp* genes by EcR is indirect (*SI Appendix*, Fig. S11). Unlike the switch in two isoforms E74, the other ecdysone-inducible early gene, broad-complex (BR-C) and Eip75 (E75), have multiple protein isoforms and complex regulatory actions (34, 35). Thus, we used the ChIP assay to examine a possible interaction of E74A and E74B to *ilp* gene promoters. The E74A genomic binding was identified at the promoters of *ilp4* and *ilp5* genes, but not detectable at *ilp8-ilp1-ilp3*, *ilp2*, *ilp6*, and *ilp7* gene promoters (*SI Appendix*, Fig. S12). We then tested the E74B isoform for binding to promoters of *ilp* genes. Such binding was enriched at the promoters of *ilp2* and *ilp6* genes but was not observed at any other *ilp* genes (*SI Appendix*, Fig. S13). Silencing of either *E74A* or *E74B* by their respective RNAi abolished binding enrichments of the respective *ilp* gene promoters (*SI Appendix*, Figs. S12 and S13).

To further confirm these results, a dual-luciferase assay was performed. When the *pAc-E74A-Myc* expression plasmid was cotransfected along with either *ilp4-Fluc* or *ilp5-Fluc* reporter plasmids, the luciferase activity was significantly higher than the control groups and *ilp6-Fluc* (Fig. 3*D* and *SI Appendix*, Fig. S10*B*). In contrast when *pAc-E74B-Myc* was cotransfected with either *ilp2-Fluc* or *ilp6-Fluc*, the luciferase activity was significantly lower than the empty vector and *ilp5-Fluc* controls (Fig. 3*E* and *SI Appendix*, Fig. S10*B*). Mutations of E74 sequence motifs in tested *ilp* gene promoters abolished the luciferase activity changes (Fig. 3 *D* and *E* and *SI Appendix*, Fig. S10*B*). Thus, these analyses indicate that the 20E/EcR pathway stimulates *ilp4* and *ilp5* genes through E74A, while suppressing *ilp2* and *ilp6* through E74B.

Regulation of ILP Protein Dynamics by the JH and 20E Pathways. In the experiments described above, we established that both JH and 20E pathways are involved in regulation of *ilp* gene expression. Effects of these pathways on ILP protein dynamics were further characterized. Insect hemolymph is a dynamic tissue and functions as an extension of intracellular environments transporting hormones (36). For total ILP levels or circulating ILP levels in hemolymph, CRISPR-Cas9-mediated homology-directed repair (HDR) and single-stranded oligodeoxynucleotides (ssODNs) were used to fuse hemagglutinin (HA) and FLAG tags into exons encoding the B- and A- chains in each of eight *ilp* genes (Fig. 4*A*). A mixture of guide RNA, Cas9 protein and ssODNs for HA tagging was delivered into wild-type (WT) eggs. The positive females with HA tag were crossed with WT males, and their offspring eggs were used for FLAG tagging. The insertion rate was recorded and verified by means of genomic PCR and Sanger DNA sequencing (*SI Appendix*, Figs. S14 and S15). Enzyme-linked immunosorbent assay (ELISA) was then performed for epitope-tagged ILP quantification using commercially available HA and FLAG monoclonal antibodies (*SI Appendix*, *Supplemental Materials and Methods*). The total content of ILPs ranged from 3 to 80 pg/mg, and their concentration in hemolymph varied from 0.2 to 90 pg/μL (Fig. 4 *B* and *C* and *SI Appendix*, Figs. S16 and S17). These analyses demonstrate that the JH and 20E pathways modulate ILP production and secretion, restricting them to appropriate amounts required during PE and PBM phases of the mosquito reproductive cycle.

The JH and 20E Pathways Antagonistically Affect FoxO Localization in the Fat Body. The insect fat body serves as a central organ for metabolism and nutrient reserve storage (37). Forkhead box O (FoxO) is one of the final transcription factors in the insulin pathway. ILPs bind to the insulin receptor (InR) and activate a signal transduction pathway and affect FoxO phosphorylation and nuclear localization (38). CRISPR-Cas9 was used to insert HA tag into the carboxy terminus of the endogenous FoxO, as previously described (28). To examine whether JH and 20E transduce their ILP effects on FoxO, we observed HA-tagged FoxO localization in fat body cells of female mosquitoes after RNAi knockdown of factors mediated by JH and 20E actions (Fig. 5 and *SI Appendix*, Fig. S18*A*). In controls, HA-tagged FoxO demonstrated nuclear localization at 72 h PE, although it was predominantly cytoplasmic at 24 h PBM, indicating the shift in FoxO activity during the vitellogenic cycle (Fig. 5). The loss of either *Met* or *Kr-h1* by RNAi in female mosquitoes with HA-tagged FoxO at 72 h PE resulted in its cytoplasmic retention (Fig. 5). In contrast, RNAi knockdown of *EcR* and *E74* at 24 h PBM caused HA-tagged FoxO nuclear translocation (Fig. 5).

To study FoxO genomic interaction with metabolic genes, we examined promoter regions of several such genes for the presence of FoxO binding sites: *succinyl-coA synthetase* (*SCS*), *trehalose-6-phosphate synthase* (*TPS*), *malate dehydrogenase* (*MDH*), *lipase*, and *fatty acid synthases* (*FAS*) (*SI Appendix*, Fig. S19). After revealing the presence of such genomic binding sites, the ChIP assay was performed to confirm the interactions of FoxO with these metabolic enzyme genes. Indeed, the FoxO-binding enrichment was observed at the promoters of these metabolic enzyme genes, which was abolished by *FoxO* RNAi silencing (*SI Appendix*, Figs. S19 and S18*B*). Moreover, *FoxO* RNAi elevated the transcripts of these metabolic enzyme genes as well as *Met*- or *Kr-h1*-RNAi, while opposite to the effects of *EcR*- or *E74*-RNAi (Fig. 6).

Discussion

The insulin signaling system is inherently complex (26). Peptide hormones and other factors affect the activity of ILPs in the regulation of multiple outcomes, such as regulation of metabolism, body size determination, development, and reproduction (25, 26). Mechanistic understanding of the transcriptional regulation of individual *ilps* is critical for revealing their actions in mosquito gonadotrophic cycles. Our present study identified that JH and 20E, the two principal hormones controlling mosquito gonadotrophic cycles, regulate ILPs, coordinating metabolism with reproduction in the disease vector mosquito *Ae. aegypti*. Moreover, our study has revealed that the JH and 20E pathways act differentially in determining the expression of the *ilp* genes. This is achieved through a direct physical interaction of JH and 20E pathway factors with promoters of *ilp* genes. Our previous CRISPR-Cas9 studies showed that *ilp2*, *ilp6*, and *ilp8* mutants are characterized by diminished fat reserves (28, 29). Depletion of either *ilp4*, *ilp5*, or *ilp7* by CRISPR-Cas9 leads to mosquito reproductive defects related to lipid homeostasis, promoting lipid storage (28, 29). Here, we have demonstrated that *ilp2*, *ilp6*, and *ilp7* are positively regulated by the JH pathway, and Kr-h1 activates the expression of these genes by directly interacting with their promoters. In contrast, the 20E pathway factor E74B inhibits the expression of *ilp2* and *ilp6* genes by directly interacting with their promoters. The situation is reversed in the regulation of *ilp4* and *ilp5* gene expression. These *ilps* are down-regulated by the JH pathway factor Kr-h1 and up-regulated by E74A through a direct interaction of these factors with promoters of these genes. Thus, both the JH and 20E pathways are involved in the expression control of the *ilp* genes, achieving coordination of their differential actions during the gonadotrophic mosquito cycle. Furthermore, we found that Met only provokes the fat body *ilp6* expression by direct binding to this *ilp* gene promoter. Thus, some regulatory proteins are specific to one *ilp* gene, some proteins act more widely, and *ilp* genes can be regulated by several factors simultaneously or at different times.

There are examples showing that expression of *ilp* genesis regulated by JH and 20E in several insect species (39–43). Juvenile hormone regulates *vitellogenin* (*Vg*) gene expression through the ILP signaling pathway in the red flour beetle, *Tribolium castaneum* (42). *Ecdysone-inducible insulin growth factor* (*IGF*)*-like peptides* in *B. mori* (*BIGFLP*) and *D. melanogaster* (*DILP6*) are predominantly expressed in the fat body (44, 45).

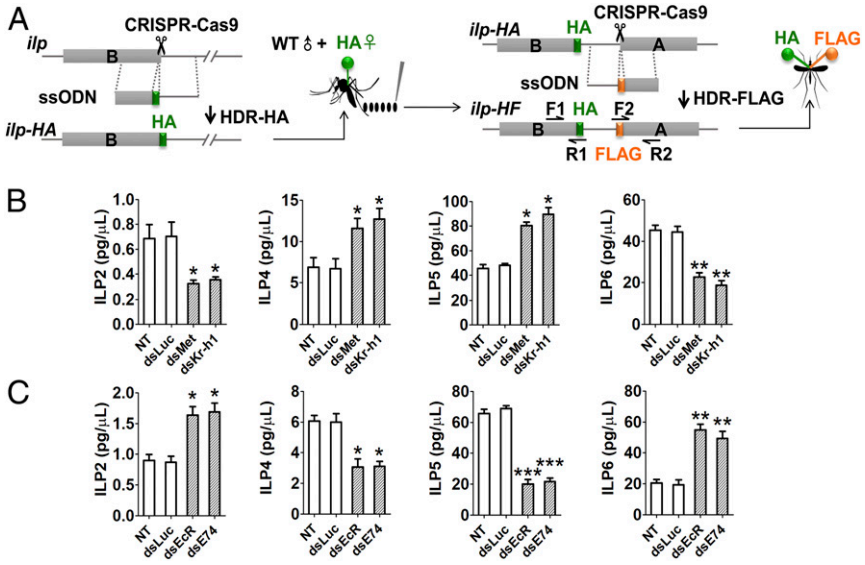

Fig. 4. CRISPR-Cas9-mediated gene tagging for the determination of hemolymph ILP levels. (*A*) Diagram indicates ILP HDR of ssODN donor bearing HA tag inserted into sequences encoding the last codon of B chain amino terminuses of each *ilp* gene to generate HA-tagged mosquito lines (*ilp-HA*). Then the eggs from HA-tagged females were used for second tagging. ssODN donor bearing FLAG tag was inserted into sequences encoding the first codon of A chain amino terminuses of each *ilp* gene to generate HA and FLAG double-tagged mosquito lines (*ilp-HF*). (*B*) Hemolymph levels of ILPs in response to JH signaling. Hemolymph ILP-HA/FLAG content (pg/μL) was determined using ELISA in tagged females after RNAi *Met* or RNAi *Kr-h1* treatments and respective controls. (*C*) Hemolymph levels of ILPs in response to 20E signaling. Hemolymph ILP-HA/FLAG content (pg/μL) was determined using ELISA in tagged females after RNAi *EcR* or RNAi *E74* treatments and respective controls. Data represent three biological replicates with five individuals in each and are shown as mean ± SEM $*P < 0.05$, $**P < 0.01$, $***P < 0.001$.

Insect ILPs differ in their secretion patterns (26, 45). We generated CRISPR-Cas9 epitope-tagged ILPs in *Ae. aegypti* to determine each ILP protein abundance. Our experimental design included tagging each of two ILP chains with either HA or FLAG. This allowed very accurate measurements of ILP protein levels using ELISA. The whole-body levels and the hemolymph circulating levels are different among ILPs. Although ILPs displayed different abnormalities in their response to RNAi of *Met*, *Kr-h1*, *EcR*, or *E74*, the set of eight ILPs was mobilized to tightly control the insulin signaling. Thus, we revealed the elements that make up the mechanisms for insulin expression, secretion, and signaling to mediate specific physiological traits in female reproducing mosquitoes.

Insect fat body is the central organ for energy metabolism, accumulating and releasing lipids and carbohydrates to meet the needs of the developing or reproducing organism. These actions are controlled by several hormones, including ILPs (33). The FoxO transcription factor is a major target of insulin action (46, 47).

In *D. melanogaster*, 20E prompts nuclear translocation of the fat body FoxO inhibiting larval growth (48). Reduced 20E signaling by RNAi-*EcR* in the larval fat body leads to increased triacyl glyceride levels (49). During pupal development, however, 20E signaling promotes adiposity (50). In female adult mosquitoes, we found the differential FoxO localization in fat body cells during two phases of the gonadotrophic cycle; FoxO was located in nuclei at 72 h PE, when the JH level is high, and in the cytoplasm at 24 h PBM, when the 20E titer is high. Knockdowns of *Met* and *Kr-h1* caused FoxO retardation in the cytoplasm, while those of *EcR* and *E74* resulted in nuclear localization. Thus, the

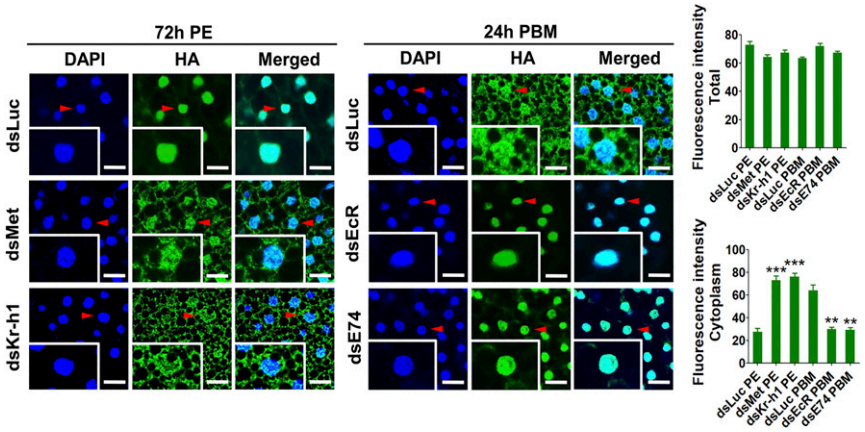

Fig. 5. FoxO subcellular localization in fat body cells. Confocal microscopic (Leica SP5) images of the fat body cells showing the FoxO-HA (green) and the DAPI signal (blue) (Scale bar: 25 μm.) *Insets* represent images of single cells. Arrowheads indicate nuclei. The mean fluorescence intensity of green signals indicates total and cytoplasmic FoxO-HA levels. Data represent three independent biological replicates with five images in each replicate and are shown as mean ± SEM $**P < 0.01$, $***P < 0.001$.

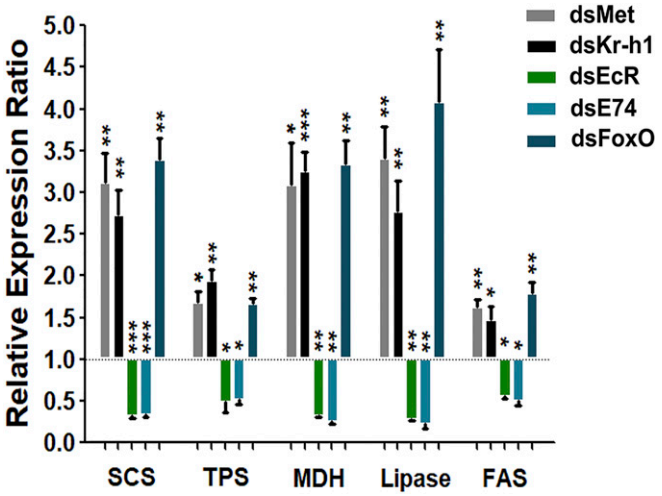

Fig. 6. Comparative analysis of transcript abundance of metabolic enzyme genes in *dsMet*, *dsKr-h1*, *dsEcR*, *dsE74*, and *dsFoxO* RNAi female mosquitoes. RNAi knockdowns of *Met*, *Kr-h1*, and *FoxO* elevated transcripts of the metabolic enzyme genes: *succinyl-coA synthetase* (*SCS*), *trehalose-6-phosphate synthase* (*TPS*), *malate dehydrogenase* (*MDH*), *lipase*, and *fatty acid synthases* (*FAS*). Knockdowns of *EcR* and *E74* repressed them. *dsLuc* (RNAi-*luciferase*) was used as control. Data represent three biological replicates and are shown as mean ± SEM $*P < 0.05$, $**P < 0.01$, $***P < 0.001$.

JH and 20E pathways act in opposite ways affecting the FoxO cellular localization and, therefore, its activity. FoxO binds and activates the *Drosophila acid lipase 4* (*dLip4*) and regulates gluconeogenesis through the activation of *phosphoenolpyruvate carboxykinase* (*Pepck*) expression (51, 52). We demonstrated FoxO binding to promoters of several carbohydrate and lipid metabolic enzyme genes in the *Ae. aegypti*.

In conclusion, we have identified a regulatory axis between ILPs and the JH and 20E pathways coordinating metabolism during gonadotrophic cycles of the disease vector, *Ae. aegypti*.

Materials and Methods

A detailed description of the materials and methods used in this paper is provided in *SI Appendix, Supplemental Materials and Methods*). *Ae. aegypti* mosquitoes and their genetics were used. RNAi, CRISPR-Cas9 knockin, gene-tagging, hormonal treatment (JH/20E), ChIP, cell luciferase, ELISA, and immunofluorescence were performed. dsRNA injection, mosquito embryo microinjection, and cell culture were previously described.

CRISPR-Cas9-Mediated Epitope Tagging. CRISPR-Cas9-mediated HDR was used to generate gene tagging. ssODN donors (199 bases) were designed (*SI Appendix*, Table S1) and synthesized as Ultramer DNA oligos (Integrated DNA Technologies) containing the 27-base HA-tag sequence or 24-base FLAG-tag sequence, flanked by homologous arms of about 86 bases. sgRNAs were designed as $N_{21}GG$ rule (*SI Appendix*, Table S1), synthesized using the MEGAscript T7 Transcription Kit (Ambion), and purified using the MEGAclear Transcription Clean-Up Kit (Ambion) following the manufacturer's protocol. Cas9 protein with nuclear localization signal was purchased (PNA Bio) and stored as 1-mg/mL reconstitutions. Preblastoderm-stage embryos were lined on filter paper, desiccated slightly, transferred onto glass slides, and microinjected with a mixture of ssODNs (125 ng/μL), Cas9 protein (333 ng/μL), and sgRNAs (40 ng/μL). Embryos were injected into the posterior pole at an angle of 10 to 25°. Injected embryos were incubated at 27 °C and 80% humidity to recover for 5 d. They were later hatched and raised to adults. Then females were crossed with wild-type males for oviposition. The females were used for PCR verification. Offspring eggs from positive females were injected for next tagging as mentioned above. The hatchlings were raised to adults. These adults (female) were subjected to RNAi (render ovary abnormalities), direct PCR (dPCR), and ELISA analysis. See *SI Appendix*, Table S1 for a list of sgRNAs and ssODN donors sequences.

Data Availability. All study data are included in the article and/or supporting information.

ACKNOWLEDGMENTS. This work was supported by NIH Grant R01AI036959 (to A.S.R.).

1. A. L. Ramírez, A. F. van den Hurk, D. B. Meyer, S. A. Ritchie, Searching for the proverbial needle in a haystack: Advances in mosquito-borne arbovirus surveillance. *Parasit. Vectors* **11**, 320 (2018).
2. M. F. Olson *et al.*, Sugar feeding patterns for *Aedes aegypti* and *Culex quinquefasciatus* (Diptera: Culicidae) mosquitoes in South Texas. *J. Med. Entomol.* **57**, 1111–1119 (2020).
3. A. D. T. Barrett, S. Higgs, Yellow fever: A disease that has yet to be conquered. *Annu. Rev. Entomol.* **52**, 209–229 (2007).
4. S. Bhatt *et al.*, The global distribution and burden of dengue. *Nature* **496**, 504–507 (2013).
5. K. A. Tsetsarkin, R. Chen, S. C. Weaver, Interspecies transmission and chikungunya virus emergence. *Curr. Opin. Virol.* **16**, 143–150 (2016).
6. C. J. McNeil, A. K. Shetty, Zika virus: A serious global health threat. *J. Trop. Pediatr.* **63**, 242–248 (2017).
7. W. A. Foster, Mosquito sugar feeding and reproductive energetics. *Annu. Rev. Entomol.* **40**, 443–474 (1995).
8. G. M. Attardo, I. A. Hansen, A. S. Raikhel, Nutritional regulation of vitellogenesis in mosquitoes: Implications for anautogeny. *Insect Biochem. Mol. Biol.* **35**, 661–675 (2005).
9. S. Roy *et al.*, Regulation of gene expression patterns in mosquito reproduction. *PLoS Genet.* **11**, e1005450 (2015).
10. M. Ashok, C. Turner, T. G. Wilson, Insect juvenile hormone resistance gene homology with the bHLH-PAS family of transcriptional regulators. *Proc. Natl. Acad. Sci. U.S.A.* **95**, 2761–2766 (1998).
11. Z. Zou *et al.*, Juvenile hormone and its receptor, methoprene-tolerant, control the dynamics of mosquito gene expression. *Proc. Natl. Acad. Sci. U.S.A.* **110**, E2173–E2181 (2013).
12. J. P. Charles *et al.*, Ligand-binding properties of a juvenile hormone receptor, Methoprene-tolerant. *Proc. Natl. Acad. Sci. U.S.A.* **108**, 21128–21133 (2011).
13. M. Li, E. A. Mead, J. Zhu, Heterodimer of two bHLH-PAS proteins mediates juvenile hormone-induced gene expression. *Proc. Natl. Acad. Sci. U.S.A.* **108**, 638–643 (2011).
14. Z. Zhang, J. Xu, Z. Sheng, Y. Sui, S. R. Palli, Steroid receptor co-activator is required for juvenile hormone signal transduction through a bHLH-PAS transcription factor, methoprene tolerant. *J. Biol. Chem.* **286**, 8437–8447 (2011).
15. T. T. Saha *et al.*, Hairy and Groucho mediate the action of juvenile hormone receptor Methoprene-tolerant in gene repression. *Proc. Natl. Acad. Sci. U.S.A.* **113**, E735–E743 (2016).
16. T. T. Saha *et al.*, Synergistic action of the transcription factors Krüppel homolog 1 and Hairy in juvenile hormone/Methoprene-tolerant-mediated gene-repression in the mosquito *Aedes aegypti*. *PLoS Genet.* **15**, e1008443 (2019).
17. F. Pecasse, Y. Beck, C. Ruiz, G. Richards, Krüppel-homolog, a stage-specific modulator of the prepupal ecdysone response, is essential for *Drosophila metamorphosis*. *Dev. Biol.* **221**, 53–67 (2000).
18. R. Ojani, X. Fu, T. Ahmed, P. Liu, J. Zhu, Krüppel homologue 1 acts as a repressor and an activator in the transcriptional response to juvenile hormone in adult mosquitoes. *Insect Mol. Biol.* **27**, 268–278 (2018).
19. T. Kayukawa *et al.*, Krüppel Homolog 1 inhibits insect metamorphosis via direct transcriptional repression of *Broad-Complex*, a pupal specifier gene. *J. Biol. Chem.* **291**, 1751–1762 (2016).
20. K. King-Jones, C. S. Thummel, Nuclear receptors–a perspective from *Drosophila*. *Nat. Rev. Genet.* **6**, 311–323 (2005).
21. S. Devarakonda, J. M. Harp, Y. Kim, A. Ozyhar, F. Rastinejad, Structure of the heterodimeric ecdysone receptor DNA-binding complex. *EMBO J.* **22**, 5827–5840 (2003).
22. J. C. Fletcher, P. P. D'Avino, C. S. Thummel, A steroid-triggered switch in E74 transcription factor isoforms regulates the timing of secondary-response gene expression. *Proc. Natl. Acad. Sci. U.S.A.* **94**, 4582–4586 (1997).
23. G. Sun, J. Zhu, C. Li, Z. Tu, A. S. Raikhel, Two isoforms of the early E74 gene, an Ets transcription factor homologue, are implicated in the ecdysteroid hierarchy governing vitellogenesis of the mosquito, *Aedes aegypti*. *Mol. Cell. Endocrinol.* **190**, 147–157 (2002).
24. K. C. Burtis, C. S. Thummel, C. W. Jones, F. D. Karim, D. S. Hogness, The *Drosophila* 74EF early puff contains *E74*, a complex ecdysone-inducible gene that encodes two *ets*-related proteins. *Cell* **61**, 85–99 (1990).
25. A. Sharma, A. B. Nuss, M. Gulia-Nuss, Insulin-like peptide signaling in mosquitoes: The road behind and the road ahead. *Front. Endocrinol. (Lausanne)* **10**, 166 (2019).
26. D. R. Nässel, J. Vanden Broeck, Insulin/IGF signaling in *Drosophila* and other insects: Factors that regulate production, release and post-release action of the insulin-like peptides. *Cell. Mol. Life Sci.* **73**, 271–290 (2016).
27. M. A. Riehle, Y. Fan, C. Cao, M. R. Brown, Molecular characterization of insulin-like peptides in the yellow fever mosquito, *Aedes aegypti*: Expression, cellular localization, and phylogeny. *Peptides* **27**, 2547–2560 (2006).
28. L. Ling, V. A. Kokoza, C. Zhang, E. Aksoy, A. S. Raikhel, MicroRNA-277 targets *insulin-like peptides 7* and *8* to control lipid metabolism and reproduction in *Aedes aegypti* mosquitoes. *Proc. Natl. Acad. Sci. U.S.A.* **114**, E8017–E8024 (2017).

29. L. Ling, A. S. Raikhel, Serotonin signaling regulates insulin-like peptides for growth, reproduction, and metabolism in the disease vector *Aedes aegypti*. *Proc. Natl. Acad. Sci. U.S.A.* **115**, E9822–E9831 (2018).
30. Y. Hou *et al*., Temporal coordination of carbohydrate metabolism during mosquito reproduction. *PLoS Genet.* **11**, e1005309 (2015).
31. X. Wang *et al*., Hormone and receptor interplay in the regulation of mosquito lipid metabolism. *Proc. Natl. Acad. Sci. U.S.A.* **114**, E2709–E2718 (2017).
32. E. Vanhandel, Metabolism of nutrients in the adult mosquito. *Mosq. News* **44**, 573–579 (1984).
33. E. L. Arrese, J. L. Soulages, Insect fat body: Energy, metabolism, and regulation. *Annu. Rev. Entomol.* **55**, 207–225 (2010).
34. P. R. DiBello, D. A. Withers, C. A. Bayer, J. W. Fristrom, G. M. Guild, The Drosophila *Broad-Complex* encodes a family of related proteins containing zinc fingers. *Genetics* **129**, 385–397 (1991).
35. J. Cruz, D. Mane-Padros, Z. Zou, A. S. Raikhel, Distinct roles of isoforms of the heme-liganded nuclear receptor E75, an insect ortholog of the vertebrate Rev-erb, in mosquito reproduction. *Mol. Cell. Endocrinol.* **349**, 262–271 (2012).
36. J. F. Hillyer, G. Pass, The insect circulatory system: Structure, function, and evolution. *Annu. Rev. Entomol.* **65**, 121–143 (2020).
37. A. S. Raikhel, "*Vitellogenesis of disease vectors, from Physiology to genes*" in *Biology of Disease Vectors*, W. C. Marquardt, Ed. (Elsevier Academic Press, 2005), pp. 329–345.
38. D. Accili, K. C. Arden, FoxOs at the crossroads of cellular metabolism, differentiation, and transformation. *Cell* **117**, 421–426 (2004).
39. N. Okamoto *et al*., An ecdysteroid-inducible insulin-like growth factor-like peptide regulates adult development of the silkmoth *Bombyx mori*. *FEBS J.* **276**, 1221–1232 (2009).
40. N. Okamoto *et al*., A fat body-derived IGF-like peptide regulates postfeeding growth in *Drosophila*. *Dev. Cell* **17**, 885–891 (2009).
41. M. Slaidina, R. Delanoue, S. Gronke, L. Partridge, P. Léopold, A *Drosophila* insulin-like peptide promotes growth during nonfeeding states. *Dev. Cell* **17**, 874–884 (2009).
42. Z. Sheng, J. Xu, H. Bai, F. Zhu, S. R. Palli, Juvenile hormone regulates vitellogenin gene expression through insulin-like peptide signaling pathway in the red flour beetle, *Tribolium castaneum*. *J. Biol. Chem.* **286**, 41924–41936 (2011).
43. R. Yamamoto, H. Bai, A. G. Dolezal, G. Amdam, M. Tatar, Juvenile hormone regulation of *Drosophila* aging. *BMC Biol.* **11**, 85 (2013).
44. A. Mizoguchi, N. Okamoto, Insulin-like and IGF-like peptides in the silkmoth *Bombyx mori*: Discovery, structure, secretion, and function. *Front. Physiol.* **4**, 217 (2013).
45. N. Okamoto, N. Yamanaka, Nutrition-dependent control of insect development by insulin-like peptides. *Curr. Opin. Insect Sci.* **11**, 21–30 (2015).
46. A. Barthel, D. Schmoll, T. G. Unterman, FoxO proteins in insulin action and metabolism. *Trends Endocrinol. Metab.* **16**, 183–189 (2005).
47. S. Lee, H. H. Dong, FoxO integration of insulin signaling with glucose and lipid metabolism. *J. Endocrinol.* **233**, R67–R79 (2017).
48. J. Colombani *et al*., Antagonistic actions of ecdysone and insulins determine final size in *Drosophila*. *Science* **310**, 667–670 (2005).
49. Y. Kamoshida *et al*., Ecdysone receptor (EcR) suppresses lipid accumulation in the *Drosophila* fat body via transcription control. *Biochem. Biophys. Res. Commun.* **421**, 203–207 (2012).
50. V. A. Francis, A. Zorzano, A. A. Teleman, dDOR is an EcR coactivator that forms a feed-forward loop connecting insulin and ecdysone signaling. *Curr. Biol.* **20**, 1799–1808 (2010).
51. J. Mattila, V. Hietakangas, Regulation of carbohydrate energy metabolism in *Drosophila melanogaster*. *Genetics* **207**, 1231–1253 (2017).
52. T. Vihervaara, O. Puig, dFOXO regulates transcription of a *Drosophila* acid lipase. *J. Mol. Biol.* **376**, 1215–1223 (2008).